The impact resistance of CTBN- modified epoxy adhesive joints

J. Lataillade, D. Grapotte, F. Cayssials

JOURNAL DE PHYSIQUE IV
Colloque C8, supplément au Journal de Physique III, Volume 4, septembre 1994

The impact resistance of CTBN- modified epoxy adhesive joints

J.L. Lataillade, D. Grapotte and F. Cayssials

LAMEF-ENSAM, Esplanade des Arts et Métiers, 33405 Talence, France

Abstract: The wide use of structural adhesives by cars'manufacturers, lays down the problem of the impact resistance of a rubber-modified epoxy-bonded steel joint. An experimental device, which allows us to reach high strain rates under different failures modes (mode I, mode II, mode I+II) and under different temperature conditions, has been developed. To allow the use of fracture mechanics, to study the substrate influence, adhesive specimens have been realized with an interfacial defect. The microstructure analysis of adhesive joints, using thermal characterization and infra-red-spectroscopy, have shown differences between joint thicknesses and between joint cures schedules, due to the hardening and phase separation processes. These morphological differences are immediately followed by modifications in energy release rate results. There is cause to believe that this phenomenon is due to the relationships between structure and mechanical properties.

Résumé: La grande utilisation des adhésifs structuraux dans l'industrie automobile pose le problème de la résistance à l'impact des assemblages collés. Cette étude a donc pour objet la détermination d'un facteur caractéristique de la résistance à l'impact d'un assemblage collé, tôle d'acier/époxy modifiée/tôle d'acier. Un dispositif expérimental nous permettant d'atteindre de grandes vitesses de déformation sous différentes températures a été développé. Afin d'étudier l'influence du substrat et de déterminer une valeur caractéristique de l'adhérence, des joints d'adhésif ont été réalisés avec une fissure interfaciale.

1. INTRODUCTION

When cured, epoxy resins are crosslinked polymers widely used as structural adhesives, especially when formulated to give a multiphase microstructure of rubbery particles in a matrix of thermoset epoxy, since this way greatly increases the toughness of the adhesive [1]. Such rubber-toughened adhesives are increasingly being used in the manufacture of vehicles and therefore their fracture behaviour under impact loading is of considerable interest. Unlike other amine curing agents, it has been found that the curing mechanism of an epoxy polymer with dycyandiamide hardener presents different pathways and shows a strong dependency on reaction temperature [2]. Moreover the CTBN-modified epoxy systems display the presence of a second rubbery phase, separated during the curing process. Various morphologies result from the competition between phase separation and hardening processes, and thus depend mainly on the nature of monomers and cures schedules. Furthermore, when it occured in an adhesive joint, the hardening reaction of such CTBN-modified epoxy systems is affected by the presence of the substrates.

The work described below was initiated to develop an instrumented device suitable for assessing the high strain rate behaviour of adhesive joints and to use a fracture mechanics approach as a method to determine the fracture energy, Gc, of adhesive joints. In order to study the influence of the substrate and especially the adhesive-substrate bonding strength, we deliberately realized an interfacial crack.

2. EXPERIMENTAL

2.1 Materials

The structural adhesive examined was an industrial one part adhesive produced by CECA Adhesifs under the trademark XEP 3374 A. The three main components of this rubber-modified are the epoxy resin (a blend of different DGEBA by-products), the curing agent (Dicyandiamide) and the rubber (a carboxyl-terminated random copolymer of butadiene and acrylonitrile). The substrate is a steel sheet XES (thickness: 0.67mm) commonly used by cars'manufacturers and referenced XES.

2.2 Preparation of adhesive joints

The adhesive joint consists of square-shaped steel sheets (40x40 mm^2) bonded by a central slip of adhesive (Fig.1). The two steel sheets were clamped together with PTFE spacers at each side to delimite the bond and to establish its desired thickness (0.2, 0.5 or 1 mm thick). Moreover, a PTFE-covered adhesive tape, stuck on the lowest sheet, allowed us to create an initial length-controlled stretched at the interface. The adhesive was cured by heating in an oven, the temperature being raised from 20°C to 150°C, maintened at 150°C for 60 minutes and then brought down to 20°C in 30 minutes. To be loaded in the impact test equipment and according to three different failures modes (mode I, mode II, mode I+II), the specimen was fixed onto supports (Fig.2). Fixation was obtained by bonding with a cyanocrylate adhesive applied to the whole surface of the steel square, which is sufficient to strongly fix it to the support.

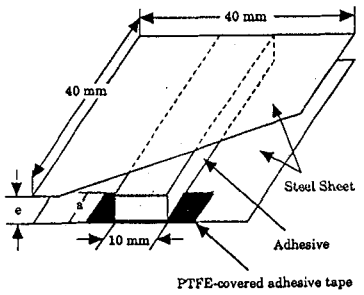

Figure 1: Schema and sizes of the adhesive joint

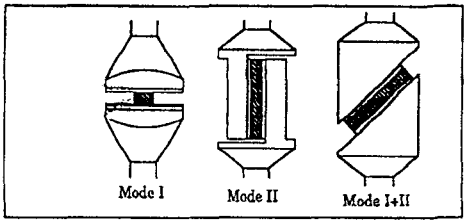

Figure 2:Modes of loading applied to adhesive joints. $\theta = 45°$ for the mode I+II

2.3 The high strain rate test equipment

The high strain rate tests were conducted using a tensile Hopkinson bar apparatus developed at the laboratory (Fig.3). In this technique, a short specimen is placed between two identical bars. The input and output bars are both 31 mm diameter Zircaloy. The input bar is 2.8 m long and the output bar is 1.9 m long. The specimen is loaded by a tensile stress wave generated in the input bar by a direct impact of a projectile tube. The duration of the test is limited by the length of the projectile that can be launched. Once the specimen is loaded, part of the loading wave propagates through to the output bar and part reflected back to the input bar. The load and deformation in the specimen are determined by monitoring the stress waves in the bars, which remain elastic during the test. By using strain-gauges and by adjusting the trigger system according to the duration of the phenomenon, the memory module is able to store the different waves. The displacement versus time history access is entrusted to an optical extensometer (Zimmer OHG). The extensometer follows the relative displacement of two targets stuck on the specimen.

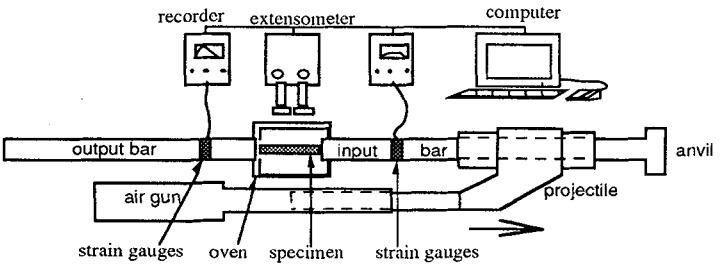

Figure 3:Schema of the tensile Hopkinson bar apparatus developed at the laboratory for adhesive joints

2.4 The fracture test

In the Hopkinson, the displacement rate of the specimen depends both on the ratio between the mechanical impedances of the bars and of the specimen and on the loading conditions. We kept two different loading conditions, denoted DYN 1 and DYN 2. Impact tests performed without specimen at the two loading conditions, DYN 1 and DYN 2, lead displacement rate values of respectively 8 m/s and 10 m/s. For these reasons, failure times have been computed for any test in order to quantify the displacement rate through the Gc parameter.

2.5 Determination of the fracture energy release rate Gc

In the present work, we have extended the energy-balance approach used by Wiliams and Kinloch in their studies about impact behaviour of polymers and adhesive joints [5-7] but with a singularity: an initial interfacial crack. In this way, Williams [5] developed a method based on the calculation of specimen fracture energy while varying the initial crack length. Especially for toughened materials with a wide plastic zone, Williams [5] showed that the fracture energy versus ligament area curves exhibited a linear variation zone (denoted zone 1 on Fig.4). The ligament area B(D-a) can be calculated from geometrical parameters (B: joint width = 10mm, D: joint length = 40mm and a: crack length). The fracture energy, U, is calculated by using the following relation, where t_f represents the failure time: $U = \int_0^{t_f} F(t)\, d\Delta(t)$

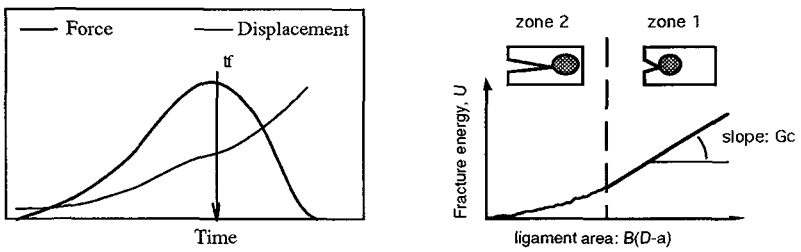

Figure 4: The force versus time and the displacement versus time recorded on the microcomputer and the theoretical feature of the fracture energy versus ligament area curve used to calculate the energy release rate, Gc, for though materials (From Williams [5])

3. RESULTS AND DISCUSSION

3.1 Differential Scanning Calorimetry

The Differential Scanning Calorimetry (DSC) provides a reliable tool for characterizing our different adhesive joints. After the hardening process, the glass transition temperatures of adhesive joints were measured by means of microcalorimeter Mettler TA 3000 DSC 30, running from -150°C to 200°C with a heating rate of 10°C/min. The results show two glass transition temperatures: TgR, glass transition temperature of the rubbery phase and TgE, glass transition temperature of the epoxy matrix. Appreciable changes are visible between the glass transition temperature values measured on the various adhesive joint thicknesses (Table II). In the curing process, the oven temperature was monitoring but the in-situ temperature was liable to variations, according to resin quantity (the reaction is exothermic, 320J/g), and because steel substrates act like radiators. For these reasons and according to bond tickness, the in-situ cure temperature was different and thus, due to the competition between phase seperation and polymerisation processes, the microstructure was different. No significant differences of TgR are noted between the 0.5 and the 0.2 mm thick bonds. Whereas the TgR of the 1 mm thick bond is twice smaller than the two other thick bonds, it is close to the TgR of the bulk specimen. The substrates influence the phase separation and the hardening process of thin bonds. Furthermore, the enthalpy of reticulationwill be all the higher as the bond will be thick.

TABLE II: The glass transition temperatures of the various bond thicknesses, determined by differential scanning calorimetry

Bond thickness	*TgR*	*TgE*
1 mm	-17°C	108°C
0.5 mm	-39°C	102°C
0.2 mm	-40°C	93°C
Bulk specimen	-20°C	100°C

3.2 Infrared Spectral Analyses

All infrared spectra were run on a Brucker IFS 113 V FTIR spectrometer. Changes in spectra were observed between the various adhesive bond thicknesses, specially the absorbency at 920,1120,1650,1740 and 2180 cm^{-1} which corresponds with IR absorption of epoxy, ether, imine, carbonyl and nitrile groups respectively [8]. The phenyl group response peak height at 830 cm^{-1} was used as internal standard in order to calibrate and compare the different samples. The relative peak heights have been gathered in Table III.

The low relative height of epoxy group response peak at 920 cm^{-1} lead us to think that we have good epoxy conversion rates (around 90%). When adhesive thickness is decreasing, reaction encourages imine and carbonyl groups development to the detriment of ether groups. Such notable variations are believed to be due to a change of reaction mechanism according to in-situ cure temperature.

TABLE III: Relative infrared absorption peak heights of main absorption peaks versus various adhesive joint thicknesses. The phenyl group response peak height at 830 cm^{-1} was used as internal standard

	830 (cm^{-1}) O - H	920 (cm^{-1}) epoxy	1120 (cm^{-1}) ether	1160 (cm^{-1}) imine	1740 (cm^{-1}) carbonyl	2180 (cm^{-1}) nitrile
1 mm thick bond	1	0.08	0.38	0.29	0.14	0.15
0.5 mm thick bond	1	-	0.29	0.28	0.24	0.09
0.2 mm thick bond	1	0.09	-	0.36	0.29	-

3.3 High strain rate tests

Experimentally, U energies were calculated from specimens with varying initial crack length (a = 5, 7.5, 10, 12.5, 15 or 20 mm). For any value of "a", five specimens were tested. A procedure of least squares fitting allowed us to determine the energy release rate, Gc (Gc: slope of the straight line). Then a criteria was applied with 90% trustworthy area in order to calculate Gc standard deviation. To quantify the displacement rate variations, according to mechanical impedance of the specimens, the $\dot{G}_c$ parameter have been used. $\dot{G}_c$ was defined as the ratio of the energy release rate over the time of failure initiation ($\dot{G}_c$ = Gc/t_f).

3.3.1 Mode I

Data are listed in Table IV. The high-level values of the fracture energies show one of the merits of the addition of a liquid rubber such as CTBN to epoxy resins. In their work, Pearson and Yee [9,10] have proved the influence of rubbery particles, and especially the particles diameters, on the toughening mechanisms. Such particles can be seen in the fracture surfaces of adhesive joints (Fig.5). It is worth to note that the particle size distribution is wide. The surface is very rough but the elastomer particles are relatively undeformed because the strain rate of the propagating crack was too high to allow significant plastic deformation and because stresses were relaxed. Fig 6 shows the effect of bond thickness on the energy release rate, GIc. It is worthly of note that the "bond thickness" is the resulting effect of the cure schedule so the results must be analysed qualitatively rather than quantitatively. The important feature is the maximum in GIc at about 0.5 mm, for both loading conditions. In the case of cohesive crack propagation, the main reason given for this [11] is that, at maximum, the plastic deformation zone size, $2r_c$, is approximetely equal to bond thickness. However, we have interfacial failure and the DSC and IR analyses, which showed bond line structure modifications according to bond thickness, incline to be cautious with this explanation. The effect of bond thickness and the role of plastic deformation are undeniable but must be balanced by the influence of microstructure modifications according to bond thickness. when the loading condition is increasing, GIc is decreasing.

TABLE IV: Results of the various adhesive joints tested in mode I under the two loading conditions

	loading condition: DYN 1			loading condition: DYN 2		
Bond thickness	GIc ($kJ.m^{-2}$)	Tf (μs)	$\dot{G}I_c$ ($kJ.m^{-2}.s^{-1}$)	GIc ($kJ.m^{-2}$)	Tf (μs)	$\dot{G}I_c$ ($kJ.m^{-2}.s^{-1}$)
1 mm	4.6±1.2	41	$1.12\ 10^5$	4.1±1.3	33	$1.24\ 10^5$
0.5 mm	6.7±0.8	51	$1.31\ 10^5$	5.3±1.4	50	$1.06\ 10^5$
0.2 mm	4.0±1.3	40	$1\ 10^5$	3.5±0.7	41	$8.5\ 10^4$

TABLE V: Results of the various adhesive joints tested in mode II under the two loading conditions

	loading condition: DYN 1			loading condition: DYN 2		
Bond thickness	GIIc ($kJ.m^{-2}$)	Tf (μs)	$\dot{G}II_c$ ($kJ.m^{-2}.s^{-1}$)	GIIc ($kJ.m^{-2}$)	Tf (μs)	$\dot{G}II_c$ ($kJ.m^{-2}.s^{-1}$)
1 mm	7.7±+1.4	47	$1.88\ 10^5$	10.8±2.3	33	$3.27\ 10^5$
0.5 mm	13.8±1.8	58	$2.37\ 10^5$	24±4.0	51	$4.7\ 10^5$
0.2 mm	11.6±2.0	43	$2.7\ 10^5$	15.6±3.2	44	$3.55\ 10^4$

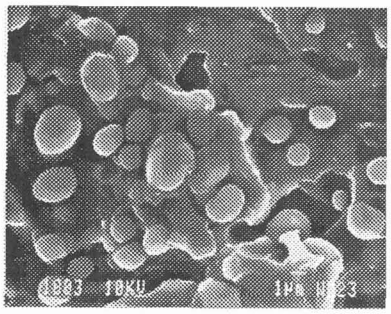

(a)

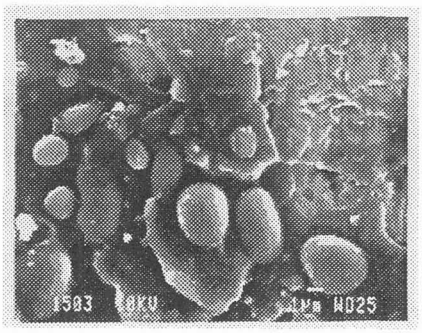

(b)

Figure 5: A Scanning Electron Microscopy of the fracture surface of a 1mm thick bond (a) and a 0.5 mm thick bond (b), tested in mode I

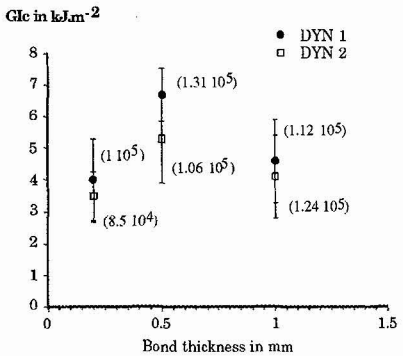

Figure 6: The GI_C vs. bond thickness curve. $\dot{G}I_C$ values in $kJ.m^{-2}.s^{-1}$ are put in brackets

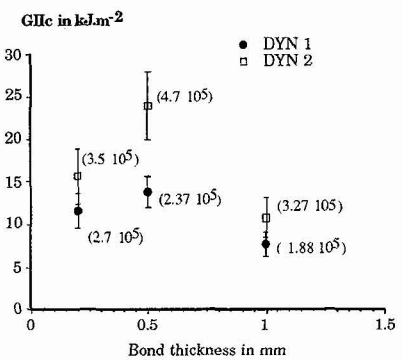

Figure 7: The GIIc vs. bond thickness curve. $\dot{G}II_C$ values in $kJ.m^{-2}.s^{-1}$ are put in brackets

3.3.2 Mode II

As shown in Table V, the adhesive joint is at least an order of magnitude tougher in shear than in tension. Unlike mode I, GIIc values increase when the loading condition moves from DYN 1 to DYN 2 since the viscoplastic contribution (internal friction of the macromolecular chains) is much more important in mode II than in mode I. The GIIc versus bond thickness curves (Fig.7) confirm the importance taken by the adhesive layer structure. In fact, the maximum value of GIIC is reached at the same bond thickness , 0.5 mm. In the failure of an adhesive joint, the rupture of chemical bonds can account for less than 10% of the measured energy [12]. Most of the fracture energy involves viscoelastic and plastic deformation of the resin structure at the crack tip. Due to this fact, the GIIc maximum can be correlated to the adhesive microstructure modifications.

3.3.3 Mode I+II

Trantina [13] has developed a design for studying joint fracture under combinations of mode I and II. This test configuration has been applied to our adhesive joint with the bond at an angle of 45° to the loading direction. High strain rate tests give values of GI+IIc (Table VI and Fig.8) lower than GIc values. This result is in agreement with low strain rate results [14]. This feature may arise because the stress-combined loading restrains the development of a large plastic zone at crack tip.

TABLE VI: Results of the various adhesive joints tested in mode I+II under the two loading conditions

	loading condition: DYN 1			*loading condition: DYN 2*		
Bond thickness	GI+IIc ($kJ.m^{-2}$)	Tf (μs)	$\dot{G}I+II_C$ ($kJ.m^{-2}.s^{-1}$)	GI+IIc ($kJ.m^{-2}$)	Tf (μs)	$\dot{G}I+II_C$ ($kJ.m^{-2}.s^{-1}$)
1 mm	2.7±0.6	43	$6.28\ 10^5$	4.7±1.0	35	$1.34\ 10^5$
0.5 mm	5.2±0.5	52	$1\ 10^5$	6.2±1.4	55	$1.13\ 10^5$
0.2 mm	2.5±0.9	47	$5.1\ 10^5$	3.2±0.8	49	$6.53\ 10^4$

3.3.4 Effect of test temperature

The energy release rate as a fonction of test temperature is shown in Fig.9. It is worth to note that in any failure mode the toughness was maximum at room temperature and a rapid fall in Gc values is observed when the temperature brings down from 20°C to 0°C. This transition temperature is about 20°C higher than the glass transition temperature determined by DSC.

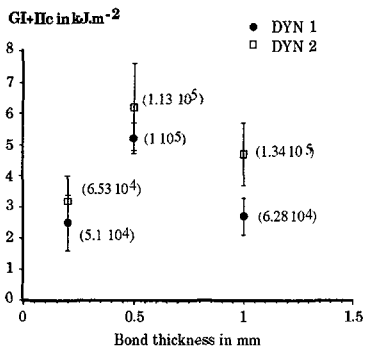

Figure 8: The GI+IIc vs. bond thickness curve. $GI+II_C$ values in $kJ.m^{-2}.s^{-1}$ are put in brackets

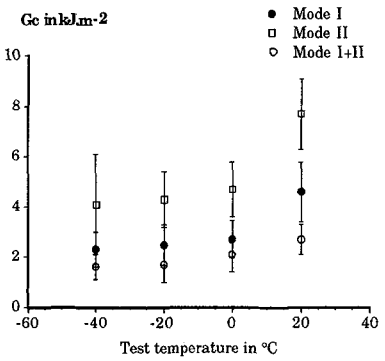

Figure 9: The energy release rate as a fonction of test temperature. The specimen is a 1 mm thick adhesive joint tested under DYN 1

4. CONCLUSION

The successful application of adhesive joint specimen to Hopkinson bar technique is the starting point to studies about adhesive joint behaviour under high strain rate loadings. A fracture mechanics approach was used to determine the energy release rate of adhesive joints tested under three different failure modes (mode I, mode II or mixed mode I+II). Dyamic tests results have shown that GI+IIc values are lower than GIc values and that GIIc values are at least an order of magnitude higher than GIc values. Beside the size parameter, the DSC and IR analyses have shown modifications in the adhesive layer structure according to bond thickness. So in any failure mode, the highest values of the energy release rate have been obtained with the 0.5 mm thick bond. Testing under such conditions, while difficult, gives data which are not possible to determine otherwise. In fact, this study is a starting point for future endeavour, especially in the area of adhesive structure determination in order to establish structure-properties relationship.

ACKNOWLEDGEMENTS

The authors would like to thank the laboratoire de Mécanique Physique of Université de Bordeaux I for its technical contribution and the Centre National de la Recherche Scientifique, the Regional Council of Aquitaine, and the CECA company, a branch of Elf-Aquitaine for their financial supports.

REFERENCES

[1] W.D. Bascom, R.Y. Ting, R.J. Moulton and A.R Siebert, *J. Mater. Sci.* **16** (1981) 2657
[2] Y.G. Lin,H. Sautereau and J.P. Pascaul,*J. Polym. Sci.* **24** (1986) 2171
[3] E.JJ Ripling, S. Mostovoy and R.L. Patrick, *ASTM STP n°360* (1971)
[4] E.J. Ripling, S. Mostovoy and H.T. Corten, *J. Adhesion* **3** (1971) 109
[5] J.G. Williams in "Fracture Mechanics of Polymers" (Ellis Horwood, Chichester, 1984)
[6] A.J. Kinloch, G.A Kodokian and M.B. Jamarani,J. *Mater. Sci.* **22** (1987) 4111
[7] A.J. Kinloch and G.A. Kodokian, *J. Adhesion* **24** (1987) 109
[8] E. Mertzel and L.Koenig, *Adv. Polym. Sci.* **75** (1986) 74
[9] A.F. Yee and R.A Pearson, *J. Mater. Sci.* **21** (1986) 2462
[10] R.A. Pearson and A.F. Yee, *J. Mater. Sci.* **21** (1986) 2475
[11] W.D. Bascom, R.L. Cottington and C.O. Timmons, *J. Appl. Polym. Sci.* **32** (1977) 165
[12] J.P. Berry in "Fracture Processes in Polymeric Solids" (Interscience, New York, 1964)
[13] G.G. Trantina, *J. Comp. Mater.* **6** (1972) 371
[14] J.N. Sultan, R.C. Laible and F.J. Mc Garry, *J. Appl. Polym. Sci.* **6** (1971) 127